BJRS

BRAZILIAN JOURNAL
OF
RADIATION SCIENCES
08-03 (2020) 01-13

Image quality evaluation for two different positron emitters in a preclinical PET scanner

[1,2]Gontijo, R.M.G., [1]Ferreira, A.V., [1,2]Souza, G.A.C., [1]Silva, J.B., [1,2]Mamede, M.

[1]Centro de Desenvolvimento da Tecnologia Nuclear/CDTN
Av. Presidente Antônio Carlos, 6.627
31270-901 Belo Horizonte, MG, Brazil
rodrigo.gontijo@cdtn.br

[2]Departamento de Anatomia e Imagem/ IMA
Universidade Federal de Minas Gerais
31270-901 Belo Horizonte, MG, Brazil

ABSTRACT

Positron emission tomography (PET) is widely used in preclinical trials, generating molecular images applied to biochemical, metabolic and functional investigation of organs and tissues. The positron emitters ^{11}C and ^{18}F are relevant for different diseases studies. However, they have different positron energies, ranges, and branching ratio. This could result in a distinct quality between the acquired PET images. Thus, the aim of this study was to evaluate differences in the image quality performance of the PET scanner (LabPET 4, GE) at Molecular Imaging Laboratory (LIM/CDTN) depending on the use of ^{18}F or ^{11}C. The study followed the guidelines of the NEMA NU 4-2008 standards and the recommended specific phantom was used in experimental procedures. The NEMA image-quality (IQ) phantom consists of 3 different regions to analyze distinct characteristics: uniformity, recovery coefficients (RCs) and spill-over rations (SOR) in air and water. The IQ phantom was filled with two different aqueous solutions (^{18}F-FDG and ^{11}C-PK11195), both activities calibrated at the beginning of acquisition (3.7MBq). The IQ phantom was placed in the center of the field-of-view (FOV) and measured with the LIM/CDTN typical whole body imaging protocol. The images were reconstructed following the LIM/CDTN standard protocol: MLEM-3D algorithm, 20 iterations, no high-resolution mode, no attenuation or scatter corrections, no post-filtering. PMOD® software was used to perform images post-processing. Uniformity test revealed that ^{11}C PET image roughness is about twice ^{18}F PET image roughness. SOR tests indicated around 15% more counts in cold volumesin ^{11}C PET image than in ^{18}F PET image. The RCs for ^{11}C were systematically lower and with higher percentage standard deviations than those for ^{18}F. This study demonstrated and quantified the best performance of PET images with ^{18}F when compared to ^{11}C. This fact must be taken into account in laboratorial practice, especially when quantitative analyzes are performed.

Keywords: **image quality, preclinical PET scanner, ^{18}F, ^{11}C.**

ISSN: 2319-0612
Accepted: 2020-08-19

1. INTRODUCTION

Positron emission tomography (PET) is widely used in preclinical trials, generating molecular images applied to biochemical, metabolic and functional investigation of organs and tissues. This imaging modality of nuclear medicine is important in the development of new radiopharmaceuticals or in studies of new applications of traditional radiopharmaceuticals [1]. Because of widespread use and commercial availability of small-animal PET scanners, the National Electrical Manufactures Association (NEMA) published its NU 4/2008 standards [2], a consistent and standardized methodology for measuring scanner performance parameters for small animal PET imaging. The publication covers the parameters spatial resolution, scatter fraction, count losses and random coincidence measurements, sensitivity, image quality, accuracy of attenuation and scatter corrections. In this sense, results of standardized measurements make possible to compare performances of different small animal PET scanners and can be used for acceptance tests of equipment [2].

Currently in Brazil, there are six centers of preclinical molecular imaging using PET routinely [3], one of them installed in the Molecular Imaging Laboratory (LIM) of Nuclear Technology Development Center (CDTN). Although most studies conducted at LIM/CDTN involve ^{18}F-labeled radiopharmaceuticals [4-9], some effort has been made in studies with ^{11}C-labeled radiopharmaceuticals [10, 11]. In this context, it is important to keep in mind that differences in physical and chemistry properties of radionuclides can results in different performances of the PET scanner [12]. For example, the positron maximum energy is about 0.6 MeV for ^{18}F and about 1.0 MeV for ^{11}C. Since the positron range increases with positron energy, the use of ^{11}C in PET studies results in a reduction of spatial resolution when compared with ^{18}F studies, which can be observed from increased blurring of images reconstructed with fixed reconstruction settings [12].

NEMA 4-2008 publication possesses an entire section (section 6) dedicated to evaluating the image capabilities of the scanner including image quality, accuracy of attenuation and scatter corrections. The purpose of these tests is to produce PET images simulating those obtained in a typical total body study of a small rodent by using a specific phantom [2]. The publication establishes that these tests shall be performed with 100 μCi (3.7 MBq) of ^{18}F during 20 min.

Therefore, the standard measurements procedures permit comparison of image capabilities of different scanners in a well stablished condition.

However, in the laboratorial practice, differences of performance of a particular PET scanner can occur due to the use of different radionuclides. So, the dependence of PET scanner performance with the radionuclide must be known to assure a correct image interpretation. Thus, the aim of this work was to evaluate, based in the NEMA NU 4-2008 standards, image capabilities of the PET scanner at LIM/CDTN using ^{18}F and ^{11}C positron emitters. The choice of these radionuclides was due to their use in the LIM/CDTN experimental preclinical studies.

2. MATERIALS AND METHODS

The experiments were carried out at the Molecular Imaging Laboratory (LIM/CDTN) and with collaboration of the Radiopharmaceutical Research and Production Unit (UPPR/CDTN), which made the ^{18}F-FDG and ^{11}C-PK1195 radiopharmaceuticals available. These radiopharmaceuticals were used in this work as sources of ^{18}F or ^{11}C positron emitters. Table 1 presents the main parameters of these two radionuclides.

Table 1: Main physical, chemical and nuclear properties of ^{18}F and ^{11}C radionuclides [13].

Radionuclide	Half-Life (min)	β^+Branch Ratio (%)	β^+ Energy (keV)		β^+ Range in water (mm)	
			Maximum	Mean	Maximum	Mean
^{11}C	20.4 min	99.8	0.960	0.386	4.2	1.2
^{18}F	109.7 min	96.9	0.634	0.250	2.4	0.6

2.1. PET scanner

The Triumph™ platform is a preclinical system dedicated for rodents imaging. The subsystem LabPET 4 consists of a stationary gantry with 1536 detectors. It employs an Avalanche Photo Diode (APD) detector ring incorporating an assembly of LYSO (Lutetium yttrium oxyorthosilicate – Lu1.9Y0.1SiO5) and LGSO (Lutetium gadolinium oxyorthosilicate – Lu0.4Gd1.6SiO5) scintillators optically coupled one after the other [14]. LabPET 1.12.1 software, provided by the scanner manufacturer, controls acquisition and reconstruction of PET images [15].

LabPET 4 images are acquired using a 250-650 keV energy window and 22 ns coincidence timing window. It provides axial field of view (FOV) of 3.7 cm and can operate in a dynamic or static mode. Coincident data are saved in list mode and can be sorted out as sinograms. More details about the LabPET 4 design and architecture are presented elsewhere [16, 17].

2.2. Image quality phantom

For imaging capabilities evaluation, the NEMA NU 4/2008 recommends a specific Image Quality (IQ) phantom. This phantom (Figure 1) is made up of polymethylmethacrylate (PMMA) with internal dimensions of 50 mm length and 30 mm diameter. It has a main chamber that communicates with five different diameters auxiliary rods (1, 2, 3, 4, and 5mm), all of which are expected to be filled with radiopharmaceutical water solution. Thus, activity concentration in any rod is the same that the one in main chamber. In addition, the IQ phantom possesses two cold chambers - one of them to be filled with air and the other one with water, both no radioactive. Details of IQ phantom are presented at NEMA 4-2008 publication [2].

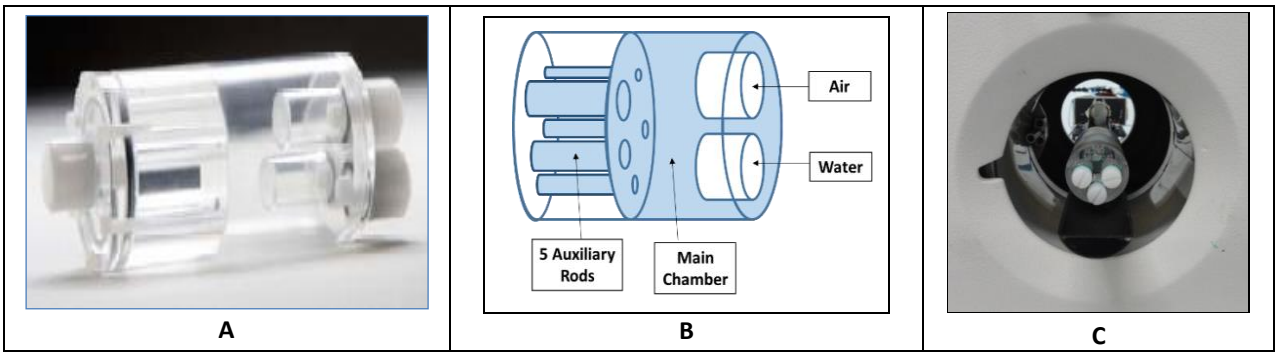

Figure 1: *Image Quality phantom.A: Photo gallery of authors; B: schematic representation where blue indicates radiopharmaceutical fillable volumes; C: phantom positioned on PET scanner FOV.*

2.1. Image Acquisition and Image Reconstruction Procedures

For ^{18}F studies, acquisition procedure and also the image analysis procedure followed the recommendation of NEMA NU 4-2008 publication (3.7 MBq at the beginning of acquisition, 20 min acquisition time). The activity in the phantom was measured with a Capintec CRC®-25R

activimeter. For ^{11}C studies, NEMA recommendations were adapted (3.7 MBq at the beginning of acquisition, 30 min acquisition time) in order to assure the same number of positrons during the image acquisition - considering half-life and branching ratio of each radionuclide.

The IQ phantom filled with radiopharmaceutical was placed in the center of the axial FOV (Figure 1C) and measured with the LIM/CDTN typical whole-body imaging protocol which uses three bed positions in order to cover the phantom length. Decay corrections were automatically done by LabPET 1.12.1 software in order to adjust the acquisition time for each bed position.

After acquisition, PET images were reconstructed following the LIM/CDTN standard protocol: MLEM-3D algorithm, 20 iterations, no high-resolution mode, no attenuation or scatter corrections, no post-filtering. IQ phantom image acquisition and reconstruction were performed with the LabPET 1.12.1 software, provided by the small-animal PET scanner manufacturer [15].

2.2. Image Analysis

After image reconstruction, scanner image capabilities tests recommended by the NEMA 4-2008 publication (section 6) were performed, namely Uniformity, Spill-Over Ratio (SOR) and Recovery Coefficient (RC):

(i) The Uniformity test consists of to obtain mean (AC_{mean}), maximum (AC_{max}), minimum (AC_{min}) and standard deviation (AC_{SD}) of the activity concentration in the main chamber. To perform this test, a central cylindrical volume of interest (VOI) with 22.5 mm diameter and 10mm height was analyzed. The number of counts per second (CPS) in the VOI were converted in activity concentration ($kBq.ml^{-1}$) using a previous calculated conversion coefficient. The percentage standard deviation (%SD), also named image roughness (%IR) [18], was evaluated according the equation (1):

$$\%SD = \%IR = 100 \times \frac{AC_{SD}}{AC_{mean}} \quad (1)$$

where: AC_{mean} is the mean activity concentration measured in VOI positioned in the uniform region of the IQ phantom and AC_{SD} is the respective standard deviation. The uniformity in the main

chamber is an indicative of attenuation and scatter correction performance of the PET scanner [2].

(ii) The ratio between the mean activity measured in a cold chamber (filled with air or water) and the mean activity measured in the main chamber provides the Spill-Over Ratio. To perform this test, a central cylindrical VOI (4 mm diameter, 7.5 mm height) in each cold chamber was analyzed. SOR test results are an indicative of scatter correction performance of the PET scanner [2].

(iii) The ratios between the mean activity measured in each one of the five auxiliary rods and the mean activity measured in the main chamber provides the image Recovery Coefficients. To perform this test, the 10 mm length central region of each rod was average to obtain a single image in which the coordinates of the highest value pixel were determined. Then, for each rod, the mean activity concentration was determined considering a 10 mm axial line passing through the highest value pixel. The RCs are indicative of the spatial resolution of the PET scanner [2].

More details of analysis for image quality tests are provided in NEMA 4-2008 and also in a previous work [9]. Image quantitative analyses were performed using PMOD® software, v3.7 [19] - software designed for research in the field of molecular imaging that allows quantitative data processing. Activity concentration in specific VOI was achieved using PMOD® PBAS tool. This tool supports viewing and processing of molecular images and allows quantitative approaches as statistics of VOI pixels [19].

3. **RESULTS AND DISCUSSION**

Figure 2 presents a comparison of typical images of IQ phantom for the two positrons emitters, ^{11}C and ^{18}F. Qualitatively, it is possible to see that ^{18}F PET image (Figure 2B) presents less image roughness and also a better IQ phantom contours definition than ^{11}C PET image (Figure 2A). This finding will be discussed further below.

Figure 3 illustrates the methodology of analysis of the PET image. In figure it is possible to see VOIs positioned in regions that were analyzed: a single cylindrical VOI in the main chamber to uniformity test (Figure 3A); three cylindrical VOIs (in main and in cold chambers) to Spill-Over Ratio tests (Figure 3B). The recovery coefficient test is illustrated for the 5mm auxiliary rod (Figure 3C).

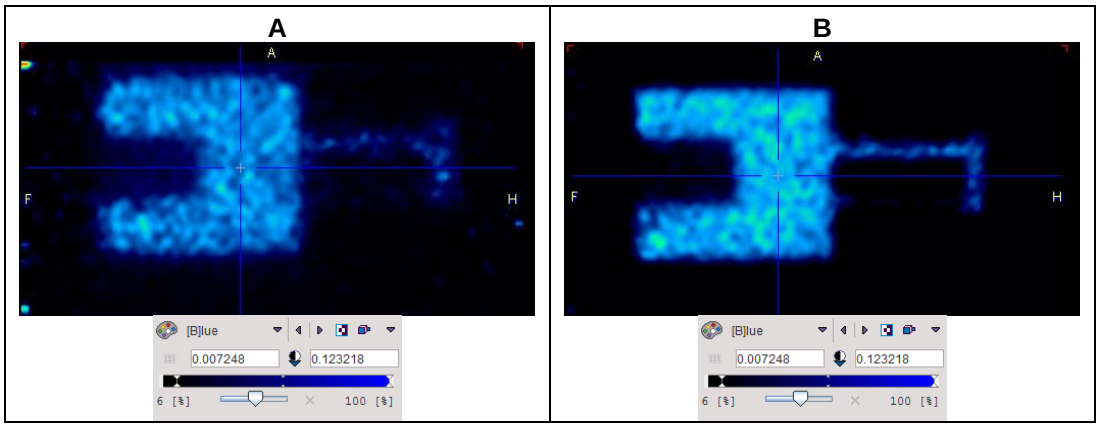

Figure 2: ***PET image (sagittal plane) of the Image Quality phantom using ^{11}C (A) e ^{18}F (B). Note that scales indicate same color definition in both images.***

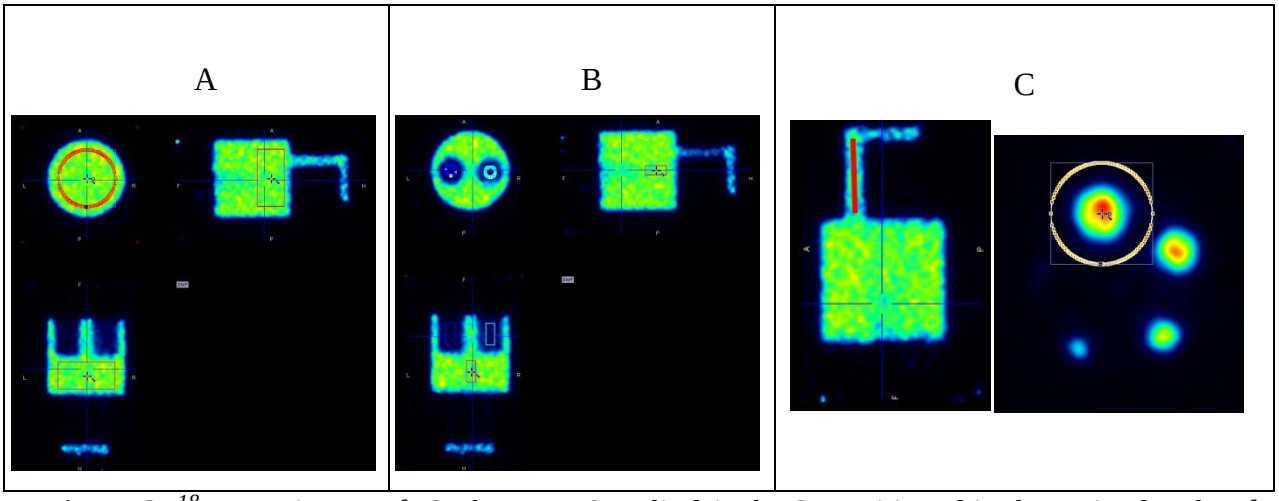

Figure 3: *^{18}F PET image of IQ phantom. A: cylindrical VOI positioned in the main chamber for Uniformity test; B: cylindrical VOIs positioned in main and cold chambers for Spill-Over Ratio tests; C: Recovery Coefficient test: (left) red line indicates the 10mm length central region of the 5mm rod; (right) orange circle indicates the average image of the 10mm length central region of 5mm rod and central cross indicates the hottest pixel.*

3.1. Uniformity test

Figure 4 presents the activity concentration in the main chamber of the IQ phantom for the two radionuclides, ^{11}C and ^{18}F.

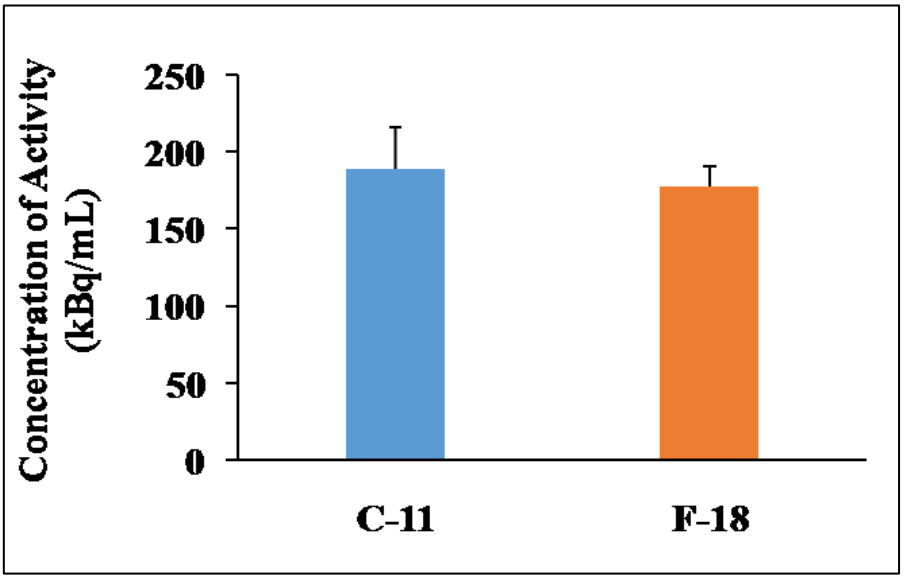

Figure 4: *Concentration of activity in IQ phantom main chamber for ^{11}C e ^{18}F.*

^{11}C PET image presented highest percentage standard deviation of the activity concentration in the main chamber of IQ phantom than^{18}F PET image: 14.5%STD for ^{11}C and 7.7%STD for ^{18}F. Considering that this parameter measures the image roughness, uniformity analysis demonstrated that ^{11}C image was twice as rough as ^{18}F image. This finding confirms the qualitative analysis of Figure 2. This fact may be explained by the higher range of ^{11}C positron when compared to ^{18}F positron range. Positron range generates an error in the localization of the true position of the positron emission since coincidence detection is related to the location of positron annihilation.

The value of image roughness for ^{18}F radionuclide obtained in this study, 7.7%, is in accordance with that published for the LabPET 8™ scanner, where the authors obtained a value of 7.0% [20]. The lack of studies using^{11}C in literature makes comparison of the performance of the PET scanner for this radionuclide with other authors and other small animal PET scanners impossible.

3.2. Spill-over ratio

Figure 5 presents the spill-over ratio in the two non-radioactive chambers (air and water) for ^{18}F and ^{11}C radioisotopes.

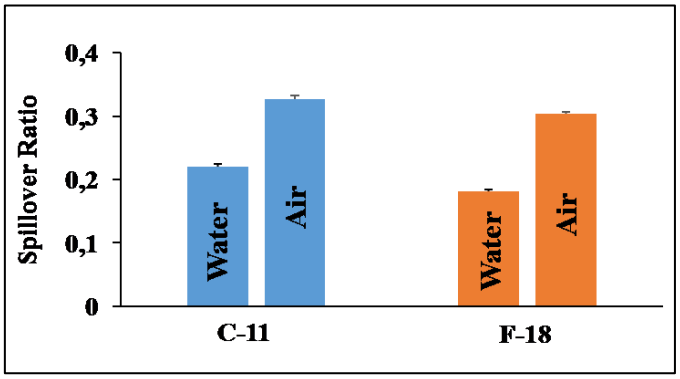

Figure 5: *Spill-over ratio for ^{11}C e ^{18}F.*

In air, the mean SOR values obtained for ^{11}C and ^{18}F were 0.33 and 0.29, respectively. In water, the mean SOR values obtained for ^{11}C and ^{18}F were 0.22 and 0.19. For both cold chambers, ^{11}C SOR values are around 15% higher than ^{18}F SOR values, indicating the worst performance of the image quality of this radionuclide. Once again, this finding is due to differences in radionuclides physical properties, since positron from ^{11}C possesses the higher positron range.

For both radionuclides, SOR values for air chamber is higher than those for water chamber. Figure 6 shows the count rates obtained from the linear profile traced in the ^{18}F PET image (axial plane) at the region containing the two cold chambers. In this figure is possible to see the difference in counting rate between water chamber and air chamber where count rates in air chamber is higher than those in water chamber.

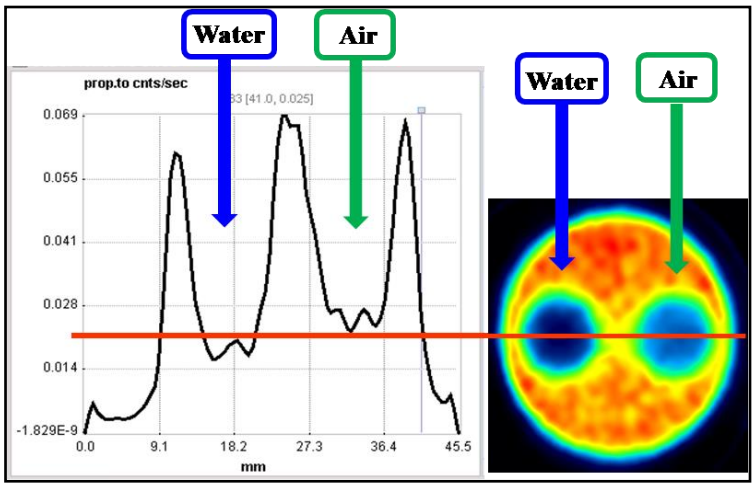

Figure 6: *^{18}F Linear profile at the region of non-radioactive chambers.*

^{18}F SOR value obtained for the cold chamber filled with water (SOR_{Water}: 0.19) are compatible with the value reported by Prasad et al. for the LabPET 8™ scanner (SOR_{Water}: 0.20)[20]. However, the^{18}F SOR value obtained for the cold chamber filled with air (SOR_{Air}: 0.29) are significantly higher than those reported by the authors (SOR_{Air}: 0.11) [20]. This fact may be explained by different characteristics between the scanners. LabPET4 scanner used in this study is not able to quantify and correct the scattered coincidence events, unlike the upper model (LabPET 8™) used by the authors [20].

The lack of studies using ^{11}C in literature makes comparison of the scanner performance of this radionuclide with other authorsand other PET scanners impossible.

3.3. Recovery coefficients

Figure 7 presents,for the two radionuclides,the recovery coefficients from the 5 auxiliary rods with different diameters (1-5mm) and respective standard deviations. Results indicate that RCs for ^{11}C were systematically lower and with higher percentage standard deviations than those for ^{18}F.

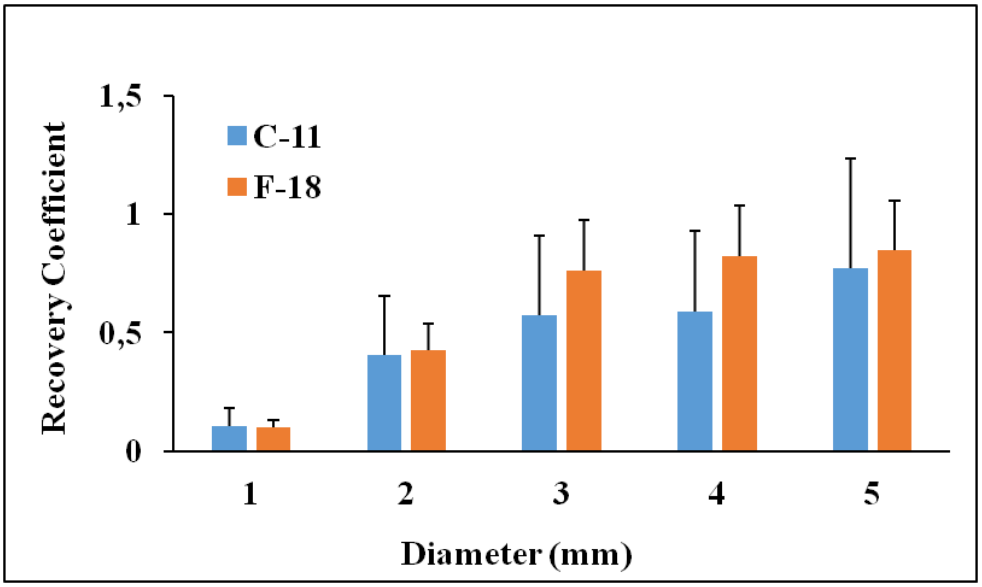

Figure 7: *Recovery coefficients from the 5 rods (1-5mm) for ^{11}C e ^{18}F.*

For the 1-mm-diameter rod, the respective RC values obtained for ^{11}C and ^{18}F were 0.10 ± 80% and 0.10 ± 30%, while for the 5-mm-diameter rod the values were 0.77 ± 60% and 0.85 ± 24%. The worst performance of ^{11}C image was expected since the RC test is an indicative of the PET scanner spatial resolution [2] and this parameter is dependent of positron range [12]. These quantitative results must be considered in PET image analysis, especially in the analysis of small structures in preclinical experiments.

RC results for ^{18}F radionuclide are in accordance with those published by Prasad et al. [20] for the LabPET 8 model: 1 mm - 0.13; 2 mm - 0.32; 3 mm - 0.58; 4 mm - 0.83; 5 mm - 0.96. The lack of studies using ^{11}C in literature makes impossible comparison of the scanner performance for this radionuclide with other authors and other small animal PET scanners.

4. CONCLUSION

The results obtained in this work using IQ phantom defined by NEMA NU 4/2008 revealed that the system LabPET 4 of LIM/CDTN produces ^{18}F PET images with performance according to the literature. The assessment of PET image quality using ^{11}C radionuclide was not found in the literature until now and makes comparison with other authors and other scanners impossible.

In a general way, it was observed that ^{18}F PET image presents better results for image quality tests when compared to ^{11}C PET image. This fact was expected due differences in radionuclides positron ranges. The present work allowed quantifying the differences in performance of the PET scanner when using these two different radionuclides. The results are important to laboratorial practice and may be taken in account in experimental preclinical study designer and also in quantitative PET image analysis.

ACKNOWLEDGMENT

This work was supported and financed by FAPEMIG, CNPq, UFMG and CDTN/CNEN. The authors would like to thank the UPPR / CDTN team for providing the radiopharmaceuticals used in the experiments.

REFERENCES

[1] R. YAO, R.; LECOMTE, R.; CRAWFORD, E. Small-Animal PET: What is it, and why do we need it?**Journal of Nuclear Medicine Technology**. Vol. 40 nº3, pp.157-165. 2011.

[2] National Electrical Manufacturers Association. **Performance Measurements of Small Animal Positron Emission Tomographs**. Rosslyn VA; 2008 Standards Publication NU 4- 2008.

[3] GONTIJO, R. M. G.; FERREIRA, A. V.; SILVA, J, B.; MAMEDE, M. Quality control of small animal PET scanner: The Brazilian Scenario. **Brazilian Journal of Radiation Sciences**. v. 8. p. 01-09. 2020.

[4] SILVEIRA, M. B. et al., Preclinical acute toxicity, biodistribution, pharmacokinetics, radiation dosimetry and microPET imaging studies of [^{18}F]Fluorocholine in mice. **Applied Radiation and Isotopes**, v. 116, p. 92-101. 2016.

[5] SILVEIRA, et al., 18 F-Fluorocholine Uptake and Positron Emission Tomography Imaging in Rat Peritoneal Endometriosis. **Reproductive Sciences**. v. 1. 2017.

[6] MENDES, B. M et al., New Radiation Dosimetry Estimates for [^{18}F]FLT based on Voxelized Phantoms. **Radiation Research**. v. 190. p. 37-44. 2018.

[7] SCHIRMER, B. G. A. et al. Comparison of [^{18}F]Fluorocholine and [^{18}F]Fluordesoxyglucose for assessment of progression, lung metastasis detection and therapy response in murine 4T1 breast tumor model. **Applied Radiation and Isotopes**. v. 140. p. 278-288. 2018.

[8] GONTIJO, R.M.G., et al. Image quality assessment using NEMA NU 4/2008 standards in small animal PET scanner. **Brazilian Journal of Radiation Sciences**. v. 7, p. 1-13. 2019

[9] GONTIJO, R. M. G., et al. Image quality evaluation of a small animal PET scanner. **Brazilian Journal of Radiation Sciences**. v. 8. p. 01-13, 2020.

[10] ALMEIDA, F. A. F., et al. Synthesis and characterization of [^{11}C]PK11195 as a PET radiopharmaceutical. In: **INTERNATIONAL NUCLEAR ATLANTIC CONFERENCE**, 2017, Belo Horizonte.

[11] OLIVEIRA, K. E. M.; MALAMUT, C.; SILVEIRA, M. B.; GONTIJO, R.M.G. Aquisição e análise quantitativa de imagens PET em camundongos sadios utilizando o radiofármaco ^{11}C-Metionina. **Curie&Roentgen**. v. 2. p. 16, 2019.

[12] IAEA - International Atomic Energy Agency. **PET/CT atlas on quality control and image artefacts**. IAEA Human Health Series no 27 (2014).

[13] IAEA - International Atomic Energy Agency. Live Chart of Nuclides. https://www-nds.iaea.org/relnsd/vcharthtml/VChartHTML.html. 2020.

[14] GE Healthcare Technologies, "**Triumph Service Guide Technical Publication**". Revision Draft 6, Copyright. http://www.gehealthcare.com 2011.

[15] Gamma Medica-Ideas. **User Manual: Positron Emission Tomography (PET) Scanner Software - Manual for Acquisition and Processing of PET Images from the LABPET System**. Software version: LABPET 1.12.0. 2010.

[16] TRETAULT, M. A. et al., System architecture of the LabPET small animal PET scanner.**IEEE Transactions on Nuclear Science**. v. 55. p. 2546-2550. 2008.

[17] FONTAINE, R. et al. The hardware and signal processing architecture of LabPET™, a small animal APD-based digital PET scanner.**IEEE Transactions on Nuclear Science**, v. 56. p. 3-9, 2009.

[18] BELCARI, N. et al., NEMA NU-4 Performance Evaluation of the IRIS PET/CT Preclincial Scanner. **IEEE Transactions on Nuclear Science.** 2017. v. 1. p. 301-309. 2017.

[19] PMOD Tecnologies LCC, PMOD v.3.7. **User Manual**. 2015.

[20] Prasad et al., NEMA NU-04 based Performance Characteristics of the LabPET-8™ Small Animal PET Scanner. **Phys. Med. Biol**. v56, p. 6649-6664. 2011.